Figure S1

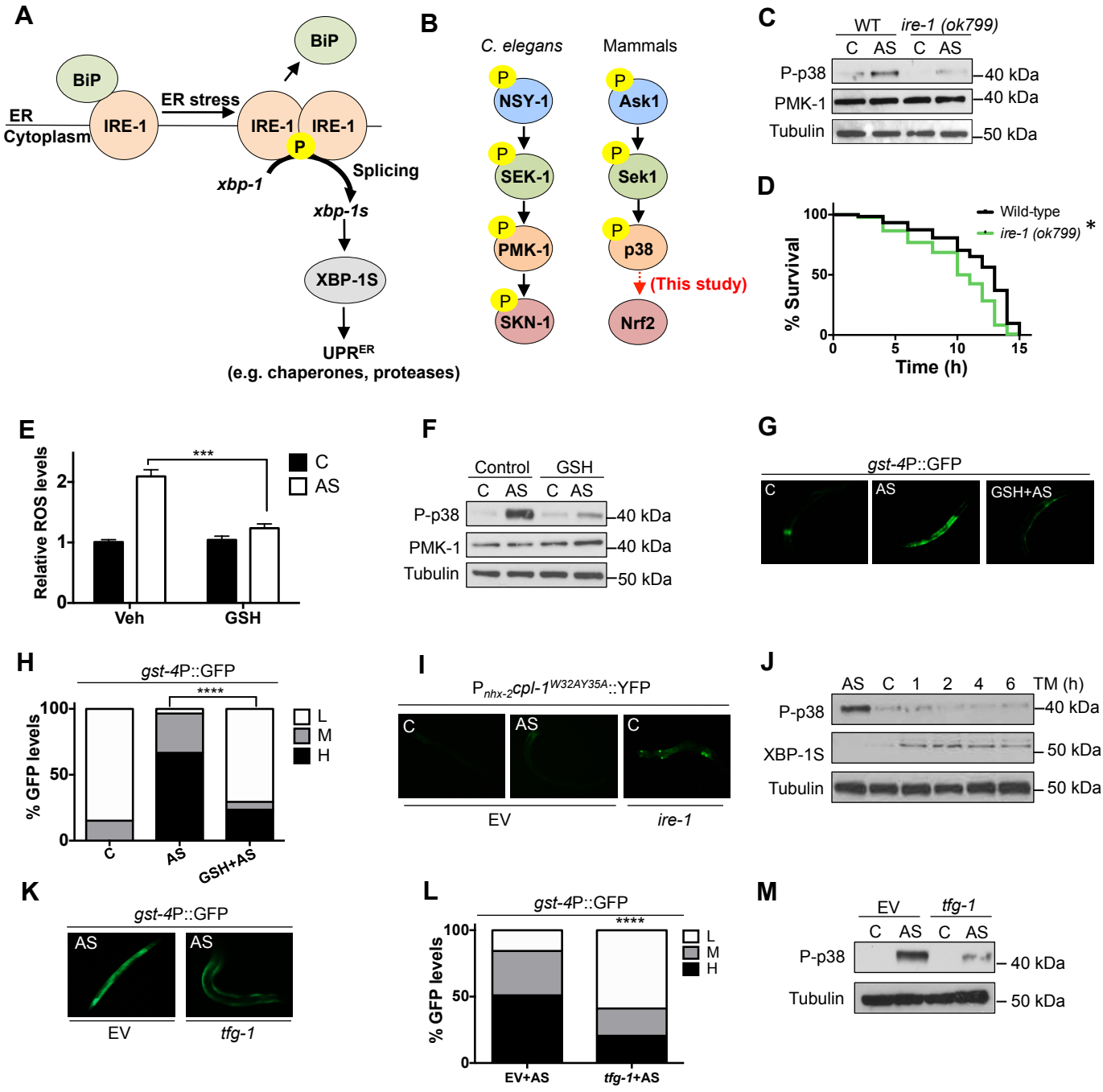
A
BiP
BiP
ER stress
ER
Cytoplasm
IRE-1
IRE-1
IRE-1
P
xbp-1
Splicing
xbp-1s
XBP-1S
UPR^ER
(e.g. chaperones, proteases)
B
C. elegans
Mammals
P
NSY-1
SEK-1
PMK-1
SKN-1
Ask1
Sek1
p38
Nrf2
(This study)
C
WT
ire-1 (ok799)
C AS C AS
P-p38
PMK-1
Tubulin
40 kDa
40 kDa
50 kDa
D
Wild-type
ire-1 (ok799)
*
% Survival
Time (h)
E
Relative ROS levels
***
C
AS
Veh
GSH
F
Control
GSH
C AS C AS
P-p38
PMK-1
Tubulin
40 kDa
40 kDa
50 kDa
G
gst-4P::GFP
C
AS
GSH+AS
H
gst-4P::GFP
****
% GFP levels
L
M
H
C
AS
GSH+AS
I
P nhx-2 cpl-1 W32AY35A ::YFP
C
AS
C
EV
ire-1
J
AS C 1 2 4 6 TM (h)
P-p38
XBP-1S
Tubulin
40 kDa
50 kDa
50 kDa
K
gst-4P::GFP
AS
AS
EV
tfg-1
L
gst-4P::GFP
****
% GFP levels
L
M
H
EV+AS
tfg-1+AS
M
EV
tfg-1
C AS C AS
P-p38
Tubulin
40 kDa
50 kDa

Figure S2

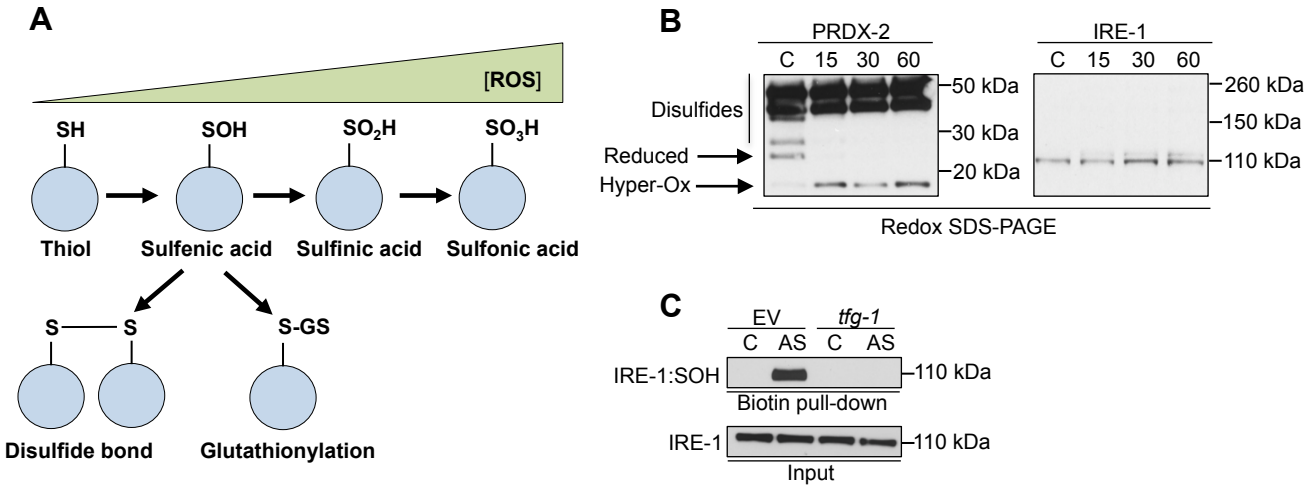
A
[ROS]
SH
SOH
SO2H
SO3H
Thiol
Sulfenic acid
Sulfinic acid
Sulfonic acid
S
S
S-GS
Disulfide bond
Glutathionylation
B
PRDX-2
C 15 30 60
IRE-1
C 15 30 60
Disulfides
Reduced
Hyper-Ox
50 kDa
30 kDa
20 kDa
260 kDa
150 kDa
110 kDa
Redox SDS-PAGE
C
EV
tfg-1
C AS C AS
IRE-1:SOH
110 kDa
Biotin pull-down
IRE-1
110 kDa
Input

Figure S3

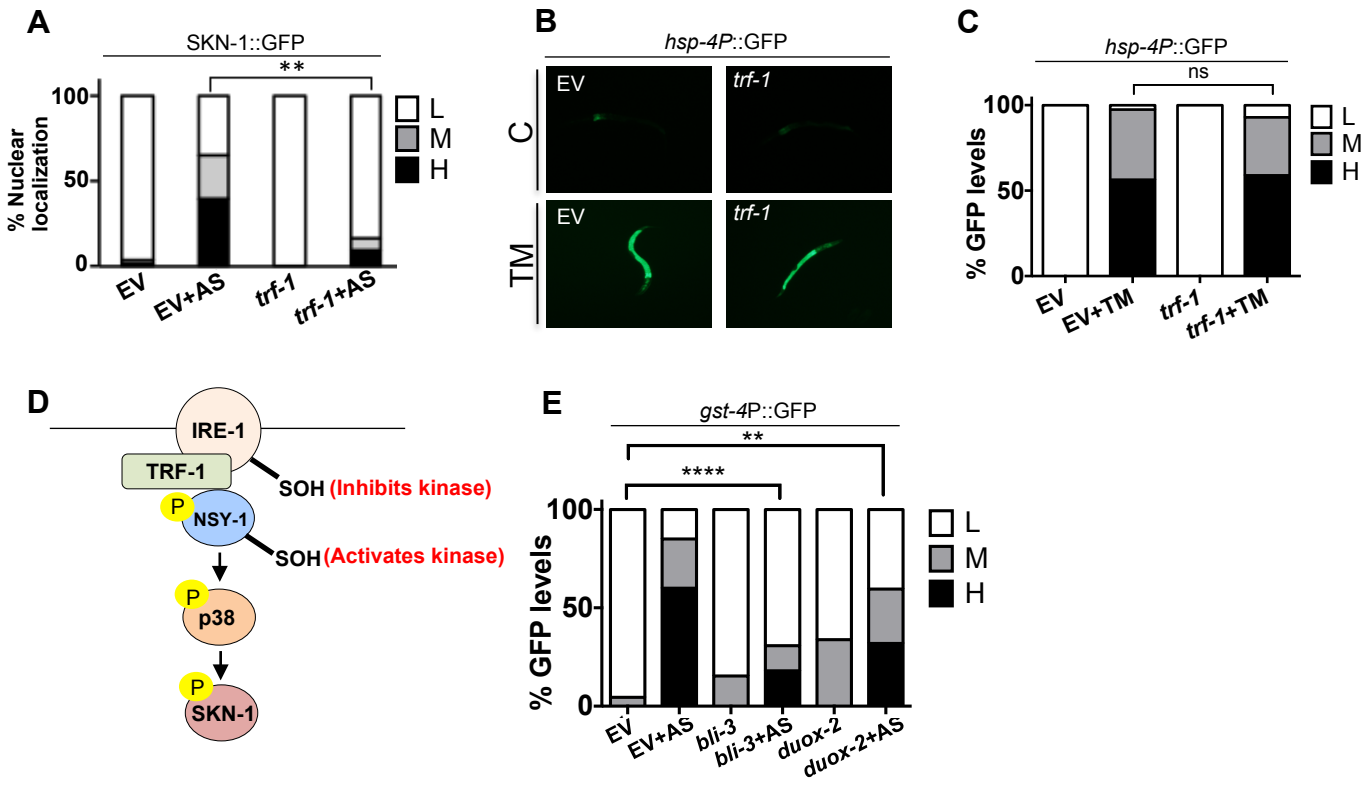
A
SKN-1::GFP
**
% Nuclear localization
100
50
0
L
M
H
EV
EV+AS
trf-1
trf-1+AS
B
hsp-4P::GFP
C
TM
EV
trf-1
EV
trf-1
C
hsp-4P::GFP
ns
% GFP levels
100
50
0
L
M
H
EV
EV+TM
trf-1
trf-1+TM
D
IRE-1
TRF-1
SOH (Inhibits kinase)
P
NSY-1
SOH (Activates kinase)
P
p38
P
SKN-1
E
gst-4P::GFP
**
****
% GFP levels
100
50
0
L
M
H
EV
EV+AS
bli-3
bli-3+AS
duox-2
duox-2+AS

Figure S4

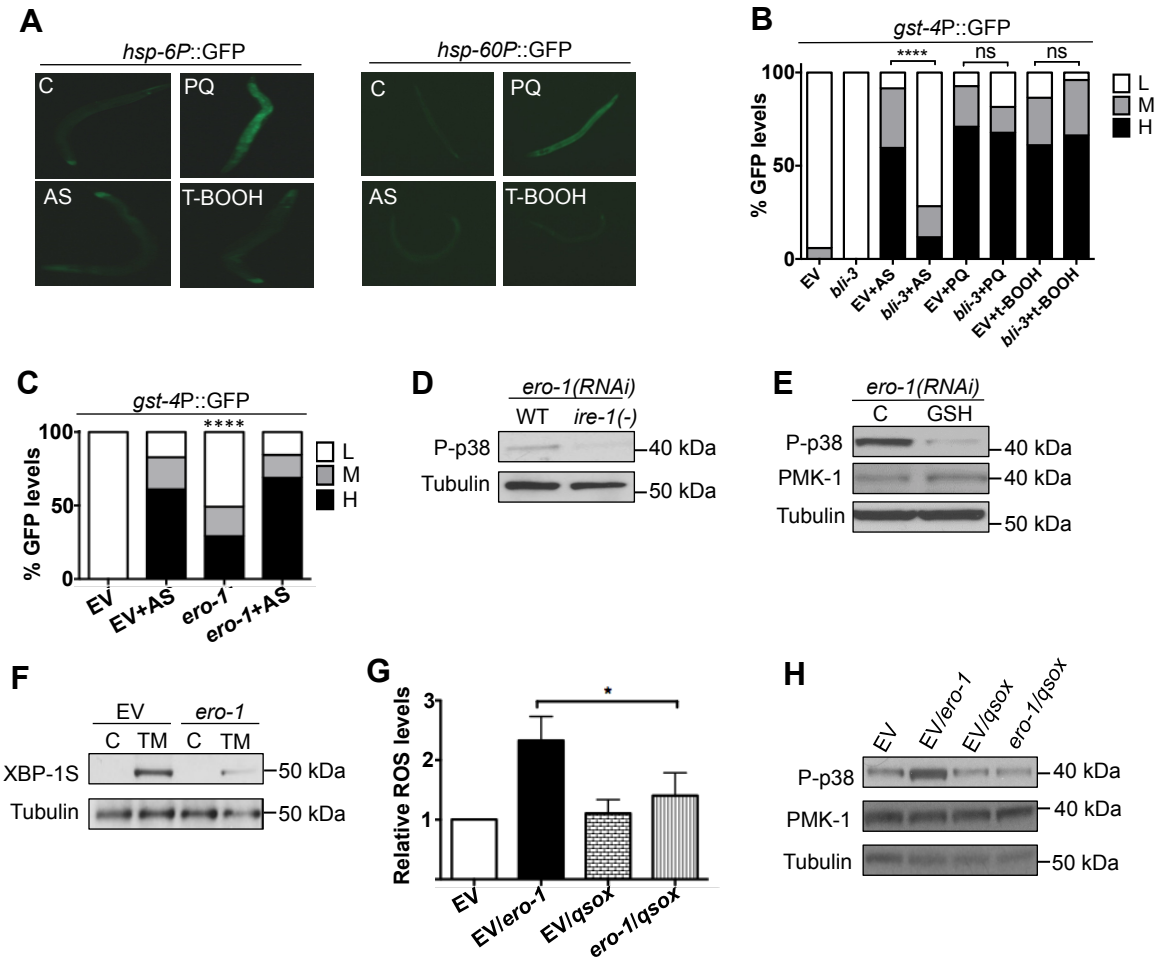
A
hsp-6P::GFP
C
PQ
AS
T-BOOH
hsp-60P::GFP
C
PQ
AS
T-BOOH
B
gst-4P::GFP
****
ns
ns
100
50
0
% GFP levels
L
M
H
EV
bli-3
EV+AS
bli-3+AS
EV+PQ
bli-3+PQ
EV+t-BOOH
bli-3+t-BOOH
C
gst-4P::GFP
****
100
50
0
% GFP levels
L
M
H
EV
EV+AS
ero-1
ero-1+AS
D
ero-1(RNAi)
WT
ire-1(-)
P-p38
40 kDa
Tubulin
50 kDa
E
ero-1(RNAi)
C
GSH
P-p38
40 kDa
PMK-1
40 kDa
Tubulin
50 kDa
F
EV
ero-1
C
TM
C
TM
XBP-1S
50 kDa
Tubulin
50 kDa
G
*
3
2
1
Relative ROS levels
EV
EV/ero-1
EV/qsox
ero-1/qsox
H
EV
EV/ero-1
EV/qsox
ero-1/qsox
P-p38
40 kDa
PMK-1
40 kDa
Tubulin
50 kDa

Figure S5

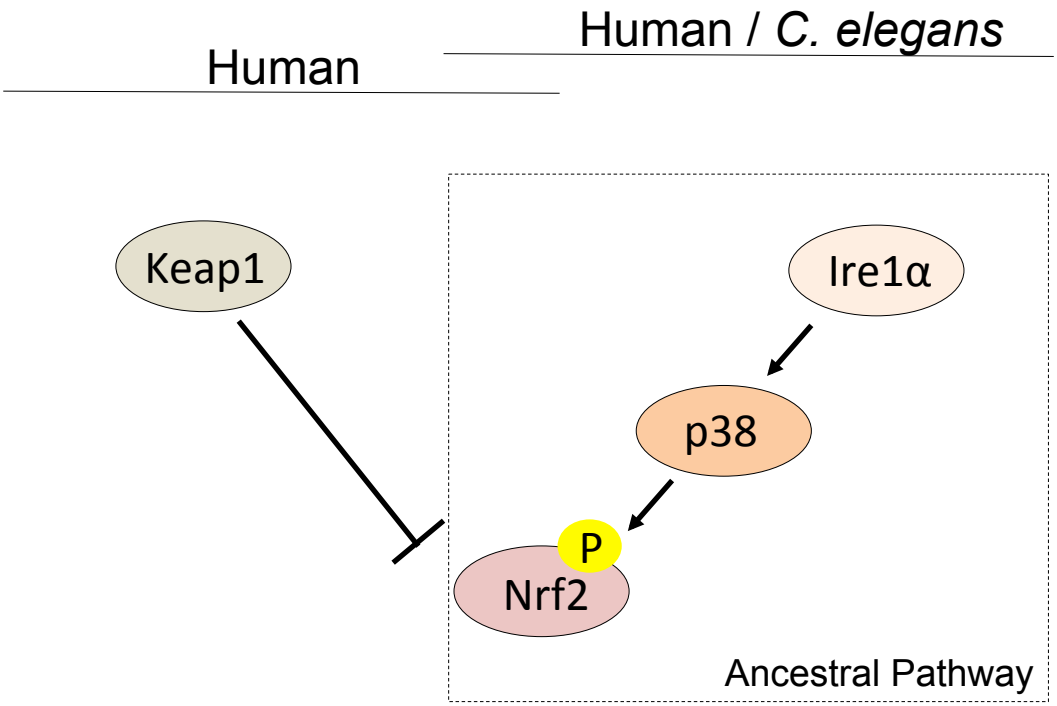
Human
Human / C. elegans
Keap1
Ire1α
p38
P
Nrf2
Ancestral Pathway

SUPPLEMENTAL FIGURE LEGENDS

Figure S1. IRE-1 responds to ROS and ER stress in a mutually exclusive manner. Related to Figure 1.

(A) Schematic of canonical IRE-1 signaling in response to ER stress. In the presence of unfolded ER proteins IRE-1 is released from the luminal chaperone BiP. **(B)** The p38/antioxidant signaling pathway in *C. elegans*, with corresponding mammalian homologs indicated. **(C)** Loss of *ire-1* reduces p38 MAPK activity. Active p38 was assessed in *ire-1 (ok799)* null animals after acute AS (30 min) treatment. **(D)** Null *ire-1(ok799)* animals are significantly more sensitive to oxidative stress (5 mM AS). **(E-H)** AS activates the p38-SKN-1 pathway by generating ROS. Treatment with the antioxidant glutathione (GSH) blocks AS-derived ROS **(E)** leading to a reduction in the p38 response to AS (30 min) **(F)**. **(G)** GSH treatment also reduced the *gst-4P*::GFP response to AS (30 min), with GFP scoring shown in **(H)**. **(I)** Acute AS treatment does not induce protein misfolding. $P_{nhx\text{-}2}cpl\text{-}1^{W32AY35A}$::YFP animals were fed either empty vector (*EV*) RNAi and treated with AS (30 min), or fed *ire-1* RNAi as a positive control. The white arrows denote the misfolded transgene. **(J)** ER stress does not activate p38 MAPK signaling. The levels of active p38 were assessed after treatment with the ER stressor TM. AS (30 min) served as a positive control. **(K-M)** *tfg-1* RNAi inhibits AS from inducing the oxidative stress response. Animals fed *tfg-1* RNAi have reduced *gst-4*P::GFP induction **(K)** in response to AS (30 min) with GFP scoring is shown in **(L). (M)** *tfg-1* RNAi reduced AS-induced p38 activity. **(H, L)** GFP quantification with high (H), medium (M) or low (L) scoring. $p < 0.0001$****; $p < 0.001$***, $p < 0.05$*. See also Table S1.

Figure S2. IRE-1 sulfenylation by ROS. Related to Figure 2.

(A) Progressive oxidation events that occur on the reactive thiol group of cysteine residues. **(B)** IRE-1 sulfenylation does not progress to disulfide bond formation. The extent of disulfide bond formation in IRE-1 was assessed by non-reducing SDS PAGE following AS treatment, using the peroxiredoxin PRDX-2 as a positive control **(Olahova et al., 2008). (C)** Induction of ER stress by *tfg-1* RNAi blocks IRE-1 sulfenylation. Animals fed *tfg-1* RNAi exhibit reduced IRE-1 sulfenylation in response to AS (30 min).

Figure S3. A local ROS signal initiates the IRE-1/p38/SKN-1 response. Related to Figure 3.

(A) *trf-1* RNAi decreases AS-induced SKN-1 nuclear localization. GFP scoring of nuclei SKN-1::GFP animals fed either control (*EV*) or *trf-1* RNAi prior to AS (30 min) treatment. **(B-C)** Knockdown of *trf-1* does not affect the UPR^{ER}. *trf-1* RNAi does not affect the activity of the *hsp-4P*::GFP reporter in response to TM (5 h) **(B)** with GFP quantification shown in **(C)**. **(D)** Schematic highlighting the ability of sulfenylation to either inactivate (IRE-1) or activate (NSY-1) kinase function. **(E)** *bli-3* and to a lesser extent, *duox-2*, is required for AS-induced *gst-4P:*:GFP activity. GFP scoring of *gst-4P*::GFP animals fed either control (*EV*), *bli-3* or *duox-2* RNAi after AS (30 min) treatment.

Figure S4. Activation of the IRE-1/p38/SKN-1 response by mitochondrial and ER-derived ROS. Related to Figure 4

(A) PQ but not AS induces mitochondrial ROS production. PQ, but not AS or t-BOOH, activates the *hsp-6P*::GFP and *hsp-60P*::GFP reporters, which are activated in the mitochondrial UPR and are surrogate biomarkers of mtROS production (see text). **(B)** *bli-3* is not required for the SKN-1 response to PQ. GFP scoring is shown for *gst-4P*::GFP animals that were fed either control (*EV*) or *bli-3* RNAi and exposed to AS (30 min), the exogenous oxidizing agent tert-butylhydroperoxide (t-BOOH) (30 min), or PQ (30 min). **(C)** Reduced *ero-1* levels increase *gst-4*P::GFP activity. **(D)** IRE-1 is required for *ero-1* RNAi-induced p38 activity. *ire-1(ok799)* animals that were fed *ero-1* RNAi show diminished active p38 compared to WT controls. **(E)** *ero-1* RNAi activates p38 through ROS production. Scavenging of ROS by GSH inhibits p38 activation by *ero-1* RNAi. **(F)** *ero-1* knockdown inhibits the IRE-1-dependent UPR^{ER}. *ero-1* RNAi decreased ER stress-induced XBP-1S production, compared to control (*EV*) samples. By contrast, *ero-1* RNAi and ER stress (TM) synergistically activated the SKN-1-driven antioxidant

response **(C)**, suggesting that TM may increase ER oxidative stress when ERO-1 levels are insufficient. **(G-H)** *ero-1* RNAi increases ROS levels **(G)** and activates p38 **(H)** in a *qsox (F47B7.2)*-dependent manner. RNAi targeting *qsox (F47B7.2)* is predicted to knock down all *qsox* isoforms because of their sequence similarity (Worm Base).

Figure S5. IRE-1 is an ancestral regulator of the Nrf2/SKN-1 antioxidant response. Related to Figure 5

(A) Cartoon highlighting the conserved role of Ire1 and p38 in regulating the Nrf2/SKN-1 antioxidant pathway independently of the Keap1/Nrf2 regulatory axis.

Table S1. Survival data for oxidative stress assays. Related to Figures S1, 2, and 3.

Set	Strain	Mean survival ± SEM (hr.)	Median Survival (hr.)	N	P value[1]
	WT; *EV (RNAi)* Control	19.8 ± 0.43	24	121	-
#1	WT; *trf-1 (RNAi)*	12.0 ± 0.38	12	117	**< 0.0001**
	WT; *EV (RNAi)*	15.2 ± 1.06	16	30	-
#2	WT; *trf-1 (RNAi)*	9.6 ± 0.88	10	32	**< 0.0001**
	WT; *EV (RNAi)*	15.9 ± 0.88	16	40	-
#3	WT; *trf-1 (RNAi)*	10.3 ± 0.85	12	40	**< 0.0001**
	WT	11.7 ± 0.28	13	140	-
#1	*ire-1(ok799*)	9.7 ± 0.28	10	134	**< 0.0001**
	WT	10.0 ± 0.76	10	50	-
	ire-1(ok799)	6.6 ± 0.56	6	36	**0.0002**
#2	*ire-1(ok799*); *ire-1P*::IRE-1^{WT} (Line 1)	9.8 ± 0.75	10	52	N.S
	ire-1(ok799); *ire-1P*::IRE-1^{C663S} (Line 1)	7.4 ± 0.61	6	64	**0.01**
	WT	10.3 ± 0.93	9	34	-
	ire-1(ok799)	7.9 ± 0.87	7	34	**0.042**
#3	*ire-1(ok799*); *ire-1P*::IRE-1^{WT} (Line 1)	10.1 ± 0.94	9	30	N.S
	ire-1(ok799); *ire-1P*::IRE-1^{C663S} (Line 1)	7.5 ± 0.76	8	31	**0.01**
	WT	11.4 ± 0.84	10	29	-
	ire-1(ok799)	7.5 ± 0.57	8	38	**0.0003**
#4	*ire-1(ok799*); *ire-1P*::IRE-1^{WT} (Line 2)	10.7 ± 1.01	10	21	N.S
	ire-1(ok799); *ire-1P*::IRE-1^{C663S} (Line 2)	7.3 ± 0.64	8	35	**0.0004**
	WT	11.1 ± 0.71	11	30	-
	ire-1(ok799)	7.1 ± 0.72	6	34	**0.0005**
#5	*ire-1(ok799*); *ire-1P*::IRE-1^{WT} (Line 2)	10.7 ± 0.71	10	28	N.S
	ire-1(ok799); *ire-1P*::IRE-1^{C663S} (Line 2)	6.8 ± 0.73	6	29	**0.0003**

Table S2. Survival data for lifespan assays. Related to Figure 4.

Set	Strain / RNAi	Mean Lifespan ± SEM (days)	Median Lifespan (days)	N (Dead/initial)	% Mean Lifespan Ext.	P value[1]
	WT; *EV (RNAi)* control	25.0 ± 0.40	26	194/215	-	-
	WT; *ero-1 (RNAi)*	29.6 ± 0.45	30	150/195	18.4	**<0.0001**
#1	*ire-1(ok799)*; *EV (RNAi)*	16.1 ± 0.24	17	248/248	-	-
	ire-1(ok799); ero-1 (RNAi)	15.5 ± 0.28	14	271/271	-3.7	0.051
	sek-1(km4); EV (RNAi)	24.2 ± 0.36	23	190/226	-	-
	sek-1(km4); *ero-1(RNAi)*	22.3 ± 0.33	23	218/245	-7.8	**0.0005**
	WT; *EV (RNAi)* control	25.5 ± 0.59	28	30/50	-	-
	WT; *ero-1 (RNAi)*	31.5 ± 0.69	33	28/69	23.5	**<0.0001**
	ire-1(ok799); *EV (RNAi)*	16.7 ± 0.50	15	51/60	-	-
#2	*ire-1(ok799)*; *ero-1 (RNAi)*	15.5 ± 0.54	15	36/58	-7.2	0.14
	sek-1(km4); EV (RNAi)	23.3 ± 0.72	23	32/60	-	-
	sek-1(km4); *ero-1 (RNAi)*	21.9 ± 0.54	23	35/62	-6	**0.02**
	WT; *EV (RNAi)* control	22.6 ± 0.51	23	49/59	-	-
	WT; *ero-1 (RNAi)*	29.1 ± 0.50	30	67/85	28.7	**<0.0001**
	ire-1(ok799); EV (RNAi)	13.4 ± 0.31	14	102/105	-	-
#3[2]	*ire-1(ok799)*; *ero-1 (RNAi)*	14.9 ± 0.38	14	81/95	11.2	**0.004**
	sek-1(km4); *EV (RNAi)*	20.6 ± 0.53	21	66/89	-	-
	sek-1(km4); *ero-1 (RNAi)*	19.6 ± 0.47	21	70/92	-4.8	0.07
	WT; *EV (RNAi)* control	20.1 ± 0.49	21	41/58	-	-
	WT; *ero-1 (RNAi)*	27.0 ± 0.65	28	38/51	34.3	**<0.0001**
#4	*ire-1(ok799); EV (RNAi)*	12.5 ± 0.34	11	61/62	-	-
	ire-1(ok799); ero-1 (RNAi)	14.3 ± 0.47	14	50/60	14.4	**0.0006**
	WT; *EV (RNAi)* control	23.1 ± 0.54	24	89/91	-	-
	WT; *ero-1 (RNAi)*	28.8 ± 0.68	27	59/89	24.7	**<0.0001**
#5	*ire-1(ok799); EV (RNAi)*	12.1 ± 0.27	12	97/99	-	-
	ire-1(ok799); ero-1 (RNAi)	11.3 ± 0.19	12	100/101	-6.6	**0.007**

	WT; *EV (RNAi)* control	24.9 ± 0.56	26	92/94	-	-
	WT; *ero-1 (RNAi)*	29.7 ± 0.57	30	72/90	19.3	**<0.0001**
#6	*sek-1(km4)*; *EV (RNAi)*	16.9 ± 0.49	20	81/84	-	-
	sek-1(km4); *ero-1 (RNAi)*	19.4 ± 0.32	20	98/98	14.8	**<0.0001**
	skn-1(zu135); *EV (RNAi)*	20.7 ± 0.58	20	43/47	-	-
	skn-1(zu135); *ero-1 (RNAi)*	12.1 ± 0.55	10	50/50	-41.5	**<0.0001**
	WT; *EV (RNAi)* control	17.9 ± 0.4	19	35/54	-	-
	WT; *ero-1 (RNAi)*	25.1 ± 1	25	27/55	40.2	**<0.0001**
	ire-1(ok799); EV (RNAi)	14.5 ± 0.23	14	72/73	-	-
#7	*ire-1(ok799)*; *ero-1 (RNAi)*	13.2 ± 0.27	14	66/69	-8.9	**0.003**
	sek-1(km4); *EV (RNAi)*	17.8 ± 0.41	20	96/96	-	-
	sek-1(km4); *ero-1 (RNAi)*	18.5 ± 0.37	20	98/98	3.9	0.6
	WT; *EV (RNAi)* control	22.8 ± 0.6	24	83/99	-	
	WT; *ero-1 (RNAi)*	33.7 ± 0.5	34	80/82	47.8	**<0.0001**
	ire-1(ok799); EV (RNAi)	11.5 ± 0.3	10	46/49	-	
	ire-1(ok799); *ero-1 (RNAi)*	10.2 ± 0.4	10	52/53	-11.3	0.02
#8	*sek-1(km4)*; *EV (RNAi)*	15.8 ± 0.2	17	187/211	-	-
	sek-1(km4); *ero-1 (RNAi)*	18.7 ± 0.2	17	167/173	18.3	**<0.0001**
	skn-1(zu135); *EV (RNAi)*	15.3± 0.5	15	30/53	-	-
	skn-1(zu135); *ero-1 (RNAi)*	13.1 ± 0.3	13	42/50	-14.4	**0.0002**
	WT; *EV (RNAi)* control	23.8 ± 0.5	25	74/88	-	
	WT; *ero-1 (RNAi)*	30.7 ± 0.8	31	52/66	29	**<0.0001**
	ire-1(ok799); EV (RNAi)	12.8 ± 0.3	11	103/106	-	
	ire-1(ok799); *ero-1 (RNAi)*	11 ± 0.3	11	69/76	-14	**0.0002**
#9[2]	*sek-1(km4)*; *EV (RNAi)*	15.2 ± 0.2	15	92/95	-	-
	sek-1(km4); *ero-1 (RNAi)*	17.9 ± 0.2	18	88/89	17.8	**<0.0001**
	skn-1(zu135); *EV (RNAi)*	18.5± 0.7	18	20/35	-	-
	skn-1(zu135); *ero-1 (RNAi)*	14.8 ± 0.3	15	46/60	-20	**<0.0001**

[1]For each experiment, P values were calculated against either *EV (RNAi)* or WT samples. In experiments 1-4, FUdR was used at 400 μM. In experiments 5-9, FUdR was used at 20 μM.

[2]These experiments are graphed in Figure 4.

SUPPLEMENTAL EXPERIMENTAL PROCEDURES

Strains
Strains were propagated on standard nematode growth medium (NGM) seeded with OP50 *E. coli* bacteria and maintained at 20°C **(Brenner, 1974)**. The wild-type strain was N2 Bristol. Other strains used in this study include: *ire-1 (ok799)*, *sek-1 (km4)*, SJ4005 *zcIs4* [*hsp-4P*::GFP], LD001 *ldIs007* [*skn-1P*::SKN-1b/c::GFP; *rol-6(su1006)*], CL2166 *dvLs19* [*gst-4P*::GFP::NLS], VK1879 *vkEx1879* [*nhx-2P*::CPL-1(W32A Y35A)::YFP + *myo-2P*::mCherry], SJ4100 *zcIs13* [*hsp-6P*::GFP], SJ4058 *zcIs9* [*hsp-60P*::GFP].

Generation of transgenic animals
cDNA constructs expressing wild-type IRE-1 from its native promoter were a kind gift from the Henis-Korenblit lab. The IRE-1^{C663S} constructs were generated using a single-site mutagenesis kit (Stratagene) and the primer 5'- CATCTCAGATTTTGGTCTTTCTAAAAGGGTTCAACCTGG-3'. To generate transgenic *C. elegans* expressing *ire-1P*::IRE-1^{WT} and *ire-1P*::IRE-1^{C663S} , *ire-1 (ok799)* animals were injected with plasmids expressing either IRE-1^{WT} or IRE-1^{C663S} at 25 ng/µl, and *rol-6 (su1006)* as a co-transformation marker at 50 ng/µl. Two independent extra-chromosomal arrays of of *ire-1P*::IRE-1^{WT} and *ire-1P*::IRE-1^{C663S} were generated and sequence-verified. Results shown are representative of each array.

RNAi feeding
RNAi experiments were performed using tetracycline-resistant HT115 bacteria expressing ampicillin-resistant dsRNA plasmids that were obtained from published libraries **(Kamath et al., 2003; Rual et al., 2004)**. RNAi cultures were grown overnight at 37°C with shaking in 5 mL LB medium containing 50 µg/mL ampicillin and 12.5 µg/mL tetracycline. Cultures were diluted 1:5 the following day in LB containing ampicillin and tetracycline and grown for 5 hours at 37°C with shaking. Cultures were centrifuged at 4,500 RPM for 20 min and supernatant was removed. Bacterial pellets were suspended in 5 mL of LB medium containing ampicillin and tetracycline, and RNAi was induced with 4 mM IPTG. Due to the severe phenotypes associated with *bli-3* RNAi, this bacterial culture was diluted 1:30 with LB media to ensure normal nematode development. Cultures were seeded onto freshly poured nematode growth medium (NGM) plates containing IPTG and allowed to dry for 48 h. Animals were bleach-synchronized and eggs or L4 stage animals were added to RNAi plates.

GFP scoring
SKN-1::GFP nuclear localization, *gst-4*P::GFP, and *hsp-4*P::GFP expression were scored as high (H), medium (M), or low (L) as described previously **(An et al., 2005; Glover-Cutter et al., 2013)**. High expression describes high GFP levels throughout all intestinal nuclei; medium expression indicates GFP levels in either the anterior or posterior intestine while low denotes weak GFP expression in intestinal nuclei. p values were calculated by two-sided Chi-square test and scoring assays were repeated at least twice.

Oxidative Stress assays
Approximately 20 worms were plated in triplicate and incubated in M9 buffer containing 5 mM sodium arsenite . Survival was scored at the indicated time points. For RNAi oxidative stress assays, Day-1 adult wild-type worms were grown on RNAi plates for three days at 20˚C and then exposed to 5 mM sodium arsenite, with survival scored hourly. p values for mean survival analysis were calculated by log-rank (Mantel-Cox) method and all assays were performed at least twice (**Table S1**).

Stress treatment
To measure XBP-1S protein levels and the induction of *hsp-4P*::GFP, synchronized L4 animals were treated on plates with 5 µg/ml Tunicamycin (TM) for 5 h. To activate p38 in *C. elegans*, L4 worms were suspended in a M9 solution containing either 5 mM sodium arsenite (AS), 50 mM paraquat (PQ), or 200 mM sorbitol (ST) and rotated for 30 mins. In *C. elegans*, responses to TM and other exogenous UPR^{ER} inducers are far slower than the response to AS **(Glover-Cutter, et al., 2013)**. To induce heat stress, worms were exposed to 35˚C on plates for 30 min. To test *gst-4*P::GFP activity, the same concentration of compound was used for 1 h. For the pre-conditioning experiments, worms were washed in M9 buffer and

allowed to recover for 30 min between treatments. For antioxidant treatment, eggs were placed on NGM plates containing 5 mM GSH and analyzed at the L4 stage. Pretreatment with 0.5 mM MitoTempo (Life Technologies), which specifically scavenges mitochondrial ROS **(Xu and Chisholm, 2014)**, was initiated 2h prior to PQ exposure. HepG2 cells were treated with 500 µM AS for 30 min or 5 µg/ml TM for 6h and fresh media was replenished after pre-treatment. p38 was inhibited with SB203580 (Sigma), NOX activity with VAS2870 (Enzo), and Ero1 with Ero1 Inhibitor II (Calbiochem).

BLI-3 activity assay
BLI-3-derived superoxide levels were measured by the lucigenin-enhanced chemiluminescence method **(ten Freyhaus et al., 2006)**. Briefly, nematodes were sonicated in lysis buffer (20 mM KH_2PO4, pH 7.0, 1 mM EGTA, 1 mM phenylmethylsulfonyl fluoride) before supernatant was added to phosphate buffer containing 5 µM lucigenin, and 100 µM NADPH. Luminescence indicative of NOX-derived ROS production was expressed relative to total protein content as determined by the BCA assay (Pierce).

Lifespan assays
Synchronized day-1 adults were placed on RNAi plates containing 5-Fluoro-2'deoxyuridine (FUdR) as indicated in Table S2, and assayed at 20°C as previously described **(Robida-Stubbs et al., 2012)**. Animals were classified as dead if they failed to respond to prodding. Exploded or bagged animals were excluded from the statistics. The log-rank method (Mantel-Cox) was used to calculate P values. (**Table S2)**.

Cell culture
HepG2 cells were grown in Dulbecco's Modified Eagle's Medium (DMEM) supplemented with 10% (v/v) fetal bovine serum, 2 mM L-glutamine, 50 units/ml penicillin and 50 µg/ml streptomycin. For transient knock-down, cells were treated with 100 µM *ire1* siRNA (Life Technologies) with RNAi MAX (Life technologies) for 72 h according to the manufacturer's instructions.

Quantiative Real-Time Polymerase Chain Reaction (qRT-PCR) Assay
Following compound treatment, RNA was extracted from synchronized adult worms using TRIzol (ThermoFisher) and cDNA was prepared using SuperScript First-Strand Synthesis superMix (ThermoFisher). mRNA levels were quantified by SYBR Green fluorescence (ThermoFisher) and analyzed by standard curve, with normalization to the geometric mean of the reference genes *cdc-42*, *pmp-3*, and Y45F10D.4. For statistical analysis, p values were calculated by a two-tailed Students *t* test.

Sulfenylation Assay
Dimedone and its derivatives have been thoroughly validated with respect to their specificity for sulfenic acid (SOH) **(Gupta and Carroll, 2014; Nelson et al., 2010; Yang et al., 2014)**. After experimental treatment, nematodes or HepG2 cells were lysed in lysis buffer [50 mM HEPES, 50 mM NaCl, 1 mM EDTA, 10% glycerol, 1% Triton x-100] supplemented with 1 mM DCP-BIO1, 0.1 mM N-ethyl malemide, 0.1 mM Iodacetamide and protease inhibitors. Samples were sonicated, kept on ice for 30 min and centrifuged at 12,000 x g for 10 min at 4˚C. The pellet was discarded and the supernatant was removed to a new tube and rotated for 1 h at room temperature to allow for labeling of sulfenic acids. After incubation, protein was precipitated by acetone to remove any excess probe and pelleted by centrifugation at 12,000 x g for 5 min. The pellet was washed in 70% acetone and suspended in non-supplemented lysis buffer. Protein levels were determined by the BCA assay and 1 mg of total protein was added to a 50 µl slurry of streptavidin beads. Then, beads were rotated over-night at 4˚C. After 24 h, beads were centrifuged at 1,000 x g for 3 min, supernatant was discarded and beads were washed in 1 ml of lysis buffer. This washing step was repeated three times and beads were eluted in 30 µl of reducing 2 x LDS buffer (Life technologies).

Co-Immunoprecipitation and western blot
C. elegans were sonicated in IP buffer (50 mM Tris-HCl (pH 7.5), 150 mM NaCl, 1 % (v/v) NP-40, 2 mM EDTA) containing protease inhibitor and kept on ice for 30 min before been centrifuged for 20 min at 13,000 x g. The supernatant (1 mg) was incubated with 2 µg of antibody overnight at 4°C. The following day, a 50 µl slurry of Protein G beads was added to the lysate for 2 hours at 4°C, after which the beads were washed three times in IP buffer and eluted in reducing 2 x sample buffer. Samples were boiled at 95˚C for 3 min, centrifuged for 1 min at 10,000 x g and loaded onto NuPAGE Novex Bis-Tris 10% Gels. Antibodies used in this study were as follows: Ire1 (Novus Biologicals), phospho-Ire1 (Novus Biologicals), Tubulin

(Cell Signaling), Ask1 (Cell Signaling), phospho-Ask1 (NSY-1) (Cell Signaling), phospho-p38 (Cell Signaling), total PMK1 (**Inoue et al., 2005**), Xbp1 (Santa Cruz), BiP (GeneTex), Nrf2 (Santa Cruz, H-300), Rock1 (Abcam), p70S6K (GeneTex), Pak1 (Abcam), Pkc-δ (Abcam), and pan-Akt (Abcam). PRDX-2 antibody was a kind gift from Dr. Elizabeth Veal (University of Newcastle, UK). All immunoblots are representative of at least two experiments (in most cases of at least three experiments). Densitometry was performed with ImageJ software. Each antibody that had been raised against a mammalian protein was chosen based upon its recognition of epitopes that are conserved in the corresponding *C. elegans* protein. The specificity of each of these antibodies was tested and validated in *C. elegans* by RNAi against the corresponding gene and immunoblotting.

ROS detection

Synchronized worms were added to a 96-well plate and incubated in 0.05 mM CM-H_2DCFDA (Life Technologies) for 1 h in the dark (**Wang et al., 2007**). After incubation, fluorescence was measured by excitation at 495 nm and emission at 520 nm. Worms were disrupted by sonication, protein concentration was determined by BCA assay (Pierce), and fluorescence was normalized to protein levels.

SUPPLEMENTAL REFERENCES

An, J.H., Vranas, K., Lucke, M., Inoue, H., Hisamoto, N., Matsumoto, K., and Blackwell, T.K. (2005). Regulation of the Caenorhabditis elegans oxidative stress defense protein SKN-1 by glycogen synthase kinase-3. Proc Natl Acad Sci U S A *102*, 16275-16280.

Brenner, S. (1974). The genetics of Caenorhabditis elegans. Genetics *77*, 71-94.

Glover-Cutter, K.M., Lin, S., and Blackwell, T.K. (2013). Integration of the unfolded protein and oxidative stress responses through SKN-1/Nrf. PLoS Genet *9*, e1003701.

Gupta, V., and Carroll, K.S. (2014). Sulfenic acid chemistry, detection and cellular lifetime. Biochim Biophys Acta *1840*, 847-875.

Inoue, H., Hisamoto, N., An, J.H., Oliveira, R.P., Nishida, E., Blackwell, T.K., and Matsumoto, K. (2005). The C. elegans p38 MAPK pathway regulates nuclear localization of the transcription factor SKN-1 in oxidative stress response. Genes Dev *19*, 2278-2283.

Kamath, R.S., Fraser, A.G., Dong, Y., Poulin, G., Durbin, R., Gotta, M., Kanapin, A., Le Bot, N., Moreno, S., Sohrmann, M.*, et al.* (2003). Systematic functional analysis of the Caenorhabditis elegans genome using RNAi. Nature *421*, 231-237.

Nelson, K.J., Klomsiri, C., Codreanu, S.G., Soito, L., Liebler, D.C., Rogers, L.C., Daniel, L.W., and Poole, L.B. (2010). Use of dimedone-based chemical probes for sulfenic acid detection methods to visualize and identify labeled proteins. Methods Enzymol *473*, 95-115.

Robida-Stubbs, S., Glover-Cutter, K., Lamming, D.W., Mizunuma, M., Narasimhan, S.D., Neumann-Haefelin, E., Sabatini, D.M., and Blackwell, T.K. (2012). TOR Signaling and Rapamycin Influence Longevity by Regulating SKN-1/Nrf and DAF-16/FoxO. Cell Metab *15*, 713-724.

Rual, J.F., Ceron, J., Koreth, J., Hao, T., Nicot, A.S., Hirozane-Kishikawa, T., Vandenhaute, J., Orkin, S.H., Hill, D.E., van den Heuvel, S.*, et al.* (2004). Toward improving Caenorhabditis elegans phenome mapping with an ORFeome-based RNAi library. Genome Res *14*, 2162-2168.

ten Freyhaus, H., Huntgeburth, M., Wingler, K., Schnitker, J., Baumer, A.T., Vantler, M., Bekhite, M.M., Wartenberg, M., Sauer, H., and Rosenkranz, S. (2006). Novel Nox inhibitor VAS2870 attenuates PDGF-dependent smooth muscle cell chemotaxis, but not proliferation. Cardiovasc Res *71*, 331-341.

Wang, S., Zhao, Y., Wu, L., Tang, M., Su, C., Hei, T.K., and Yu, Z. (2007). Induction of germline cell cycle arrest and apoptosis by sodium arsenite in Caenorhabditis elegans. Chem Res Toxicol *20*, 181-186.

Xu, S., and Chisholm, A.D. (2014). C. elegans epidermal wounding induces a mitochondrial ROS burst that promotes wound repair. Dev Cell *31*, 48-60.

Yang, J., Gupta, V., Carroll, K.S., and Liebler, D.C. (2014). Site-specific mapping and quantification of protein S-sulphenylation in cells. Nature communications *5*, 4776.